

# Electron energy spectrum produced by stochastic acceleration in the laser–plasma interaction

E. KHALILZADEH,<sup>1,2</sup> A. CHAKHMACHI,<sup>1</sup> AND J. YAZDANPANAHI<sup>1</sup>

<sup>1</sup>The Plasma Physics and Fusion Research School, Nuclear Science and Technology Research Institute, Tehran, Iran

<sup>2</sup>Department of Physics, Kharazmi University, 49 Mofateh Avenue, Tehran, Iran

(RECEIVED 13 December 2016; ACCEPTED 23 January 2017)

## Abstract

In this paper, the electrons energy spectrum produced by stochastic acceleration in the interaction of an intense laser pulse with the underdense plasma is described by employing the fully kinetic 1D-3 V particle-in-cell simulation. In this way, two finite laser pulses with the same length 200 fs and with two different rise times 30 and 60 fs are typically selected. It is shown that the maximum energy of electrons in the laser pulse with the short rise time (30 fs) is about eight times greater than the maximum energy of the electrons with the long rise time (60 fs). Furthermore, unlike the pulse with the short rise time, the shape of energy spectrum and the electrons temperature in the long rise time laser pulse are approximately unchanged over the time. These results originated from the fact that in the case of long rise time laser pulse, all electrons are accelerated by the one chaotic mechanism because of the scattered fields generated in the plasma, but in the case of short rise time laser pulse, three different mechanisms accelerate the electrons: first, the stochastic acceleration because of the nonlinear wave breaking via plasma–vacuum boundary effect; second, the stochastic acceleration initiated by the wave breaking; and third, the direct laser acceleration of the released electrons.

**Keywords:** Chaos; Electron energy spectrum; Laser–plasma interaction; Particle-in-cell simulation; Stochastic acceleration

## 1. INTRODUCTION

The rapid advances in the generation and amplification of ultra-short laser pulses (Strickland & Mourou, 1985; Mourou *et al.*, 1998) have led to the laser–plasma interaction is one of the most motivating topics in physics. In this context, electron acceleration by intense laser fields in plasmas has recently attracted a vast number of attentions due to the advent of high-power laser pulses and their potential applications. Different acceleration mechanisms have been proposed, including the wakefield acceleration (Ting *et al.*, 1997; Litos *et al.*, 2014), the direct laser acceleration (Li *et al.*, 2011; Shaw *et al.*, 2014; Zhang *et al.*, 2015) and electron acceleration due to the stochastic motion of electrons (Sheng *et al.*, 2002; Zhang *et al.*, 2003a, b; Sheng *et al.*, 2004; Paradkar *et al.*, 2011; Khalilzadeh *et al.*, 2015). In the last case, electrons can be accelerated significantly far beyond the ponderomotive potential level of the incident pulse.

The motion of single electrons in a plane electromagnetic wave is integrable (Sarachik & Schappert, 1970). However, if there is a perturbation to electron motion in this plane wave, such as another plane wave, a magnetic field, or a stochastic field, the corresponding Hamiltonian cannot be integrable (Smith & Kaufman, 1975; Escande & Doveil, 1981; Lichtenberg & Lieberman, 1981; Mendonca, 1983; Bauer *et al.*, 1995). In this case, acceleration of electrons to much higher energy is possible. Stochastic acceleration could be responsible for the high-energy electrons generation observed in the previous simulation and experimental works (Adam *et al.*, 1997; Tzeng *et al.*, 1997; Zhang *et al.*, 2003a, b; Yazdani *et al.*, 2014). Sheng *et al.* (2002, 2004) have shown that stochastic acceleration of electrons in vacuum and underdense plasmas by an intense laser pulse can be triggered in the presence of another counter-propagating or intersecting laser pulse. The other particle-in-cell (PIC) simulation results (Khalilzadeh *et al.*, 2015) indicate that the amplitude of backscattered fields in proper long pulse length can be high enough to act as a second counter-propagating wave and generates the electrons with high energy and high temperature.

Address correspondence and reprint requests to: E. Khalilzadeh, The Plasma Physics and Fusion Research School, Nuclear Science and Technology Research Institute, Tehran, Iran and Department of Physics, Kharazmi University, 49 Mofateh Avenue, Tehran, Iran. E-mail: [el\\_84111005@aut.ac.ir](mailto:el_84111005@aut.ac.ir)

However, the previous numerical studies on the stochastic acceleration have been limited to the high-energy electrons generated in the presence of two electromagnetic waves, in which the second wave can be either a laser pulse or the scattered fields generated in the plasma (Sheng *et al.*, 2002; Zhang *et al.*, 2003a, b; Sheng *et al.*, 2004; Paradkar *et al.*, 2011; Khalilzadeh *et al.*, 2015). On the other hand, in the interaction of a high-intensity laser pulse with underdense plasma, with considering the full plasma reaction, the new electromagnetic and the longitudinal electrostatic waves are produced. In this case, it is expected that the high-energy electrons can be generated through other chaotic mechanisms. In this paper, we describe the electron energy spectrum produced by different chaotic mechanisms in the laser–plasma interaction by employing the fully kinetic 1D-3V PIC simulations. Two finite laser pulses with the same length and with two different rise times are typically selected. It is illustrated that the maximum energy of electrons in the laser pulse with short rise time has the higher amount; it is about eight times greater than the maximum energy of electrons in the laser pulse with long rise time. Furthermore, the shape and the mean broadening of the energy spectrum in the long rise time case are approximately unchanged over the time. This shows that in the interaction of the plasma with the long rise time laser pulse, all electrons are affected by the one acceleration mechanism. In this case, the amplitude of the scattered wave and the incident wave can satisfy Mendonca stochastic criteria (Mendonca, 1983), for the occurring the chaos. If the rise time of the pulse is short, chaos mechanism is initiated by the space-charge wave breaking. In this case, some of the electrons, which are released because of the wave breaking are accelerated to the very high energies by the laser pulse field, directly. These electrons remain in the tail part of the electron distribution function over the time. Generally, three mechanisms accelerate the electrons over the time in the short rise time laser pulse: the chaotic mechanism originated from the nonlinear wave breaking via plasma-vacuum boundary effect, the chaotic mechanism because of the wave breaking, and the direct laser acceleration of the released electrons. Therefore, the phase space pattern and the shape and mean broadening of the energy spectrum change over the time. Also, in agreement with chaotic nature of the motion, it is found that the electrons energy will considerably be changed by applying a minor change to the initial laser or plasma parameters.

This paper is organized in different sections. In Section 2, the physical description of chaotic motion is considered using the Lagrangian of the single electron in the electromagnetic fields. In Section 3, the electron energy distribution extracted from our PIC simulations is described. The parametric analyses are done by varying the laser intensities and the plasma densities in Section 4. Finally, in Section 5, the paper is concluded.

**2. THEORY**

The motion of single electron in a plane electromagnetic wave  $[A_1(x, t)]$  is integrable. In the presence of another

plane electromagnetic wave  $[A_2(x, t)]$ , the Lagrangian of the electron is (Jackson, 1962):

$$L_0 = -m_q c^2 \sqrt{1 - \frac{v^2}{c^2}} + \frac{q}{c} [V \cdot (A_1(x, t) + A_2(x, t))], \tag{1}$$

where,  $m_q$ ,  $c$ ,  $V$ , and  $q$  are the mass electron, speed of light, electron velocity, and electron charge, respectively. In this case, the motion of the particle can be chaotic provided that the Mendonca criterion  $a_1 a_2 = 1/16$  ( $a_1$  and  $a_2$  are the normalized vector potential) is satisfied (Mendonca, 1983). In the interaction of a high-intensity laser pulse with underdense plasma, because of the full plasma reactions, the self-consistent fields in the plasma can produce new electromagnetic and longitudinal electrostatic waves. Therefore, the Lagrangian of the single electron in the plasma is:

$$L = -m_e c^2 \sqrt{1 - \frac{v^2}{c^2}} + \frac{q}{c} [V \cdot A(x, t)] - q\phi(x, t), \tag{2}$$

that  $A(x, t) = \sum_i A_i(x, t)$ , where  $A_i(x, t)$  is the component of electromagnetic radiations (scattered and incident waves) and  $\phi(x, t) = \sum_i \phi_i(x, t)$ , where  $\phi_i(x, t)$  is the component of the scalar potential. Two scalar potentials generated in the laser–plasma interaction are  $\phi_w(x, t)$  and  $\phi_{th}(x, t)$ . Here  $\phi_w(x, t)$  is the space charge potential, wake potential in one dimension (Sprangle *et al.*, 1990), and  $\phi_{th}(x, t)$  is the thermal Langmuir wave potential (Bulanov *et al.*, 1998). In fact, when the laser pulse propagates in the plasma, the wake wave breaks due to the inhomogeneity of the density on the vacuum-plasma surface. This nonlinear wave breaking produces a new off-phase potential  $[\phi_{th}(x, t)]$ . In one dimension, consider one laser field in interaction with the plasma. In this case, a frame can be found, so that in which quasi-static approximation is established. In fact, this frame travels with group velocity of the laser field (commoving frame). In the quasi-static situation, the fields  $a$  ( $a$  is normalized vector potential) and  $\phi_w$ , which derives the plasma wave are expected to be constant during a transit time of the plasma through the laser field. Under quasi-static approximation in the commoving frame, plasma wave generation is described by

$$\frac{\partial^2 \phi_w}{\partial \xi^2} = k_p^2 \left[ \frac{n}{n_0} - 1 \right] = \frac{k_p^2}{2} \left[ \frac{1 + a^2}{(1 + \phi_w)^2} - 1 \right], \tag{3}$$

where  $\xi = x - v_{gr}t$  ( $v_{gr}$  is the group velocity of the laser field),  $k_p^2 = 4\pi n_0 q^2 / m_e c^2$  ( $n_0$  is the equilibrium electron density), and  $\phi_w = q\phi_w / m_e c^2$  is the normalized wake potential (Sprangle *et al.*, 1990). For example in the short pulse limit, when  $|\phi_w| < 1$  this equation can be solved for arbitrary laser field as:

$$\phi_w = \frac{k_p}{2} \int_{\zeta}^0 a^2(\zeta') \sin(\zeta' - \zeta) d\zeta'. \tag{4}$$

If in Eq. (2) one of the potentials that has proper phase relation

with other potentials is greater than the others, the electron is mainly affected by this potential and the system is integrable. Otherwise, it is expected that the electron motion can be chaotic through different chaotic mechanisms. In fact, when the chaos occurs, the electron cannot choose one of the defined paths. Each potential with a distinct phase specifies a clear path for the electron. Depending on the initial conditions, the electron chooses one of these different paths and can travel from one path to the other. In this case, the maximum kinetic energy of electrons cannot be determined, and acceleration of electrons to much higher energy is possible. Since the analytical study of this issue is not possible, we use PIC simulation in the next section to obtain precise results for the electron energy in the light of the mentioned factors.

### 3. SIMULATION RESULTS AND DISCUSSION

To avoid the repeating of simulation parameters through this section, the simulation parameters are summarized here. These simulations are conducted using the code 1D-3V PIC (Yazdanpanah & Anvary, 2012; Yazdanpanah & Anvary, 2014), which includes the physics of ionization (Khalilzadeh *et al.*, 2016). The laser wavelength has invariantly been considered  $\lambda = 1 \mu\text{m}$  in all the cases. For all run-instances, we have used hydrogen atoms with initial profile that have been step-like. High spatial resolution of 200 cells per laser wavelength with at least 64 particles per cell is used in the simulations. The spatial resolution guarantees the plasma against the un-physical heating produced by the finite-grid instability by appropriate resolution of the Debye length  $\lambda_D$ , that is,  $DX/\lambda_D \approx 0.3$ . The size of simulation box is  $600\lambda$  with open and reflective boundary conditions being applied at its ends for the fields and particles, respectively. The laser intensity and the density of hydrogen atoms are  $I = 10^{18} \text{ w/cm}^2$  and  $n = 0.02 n_{cr}$ , respectively. The pulse envelope consists of three parts: flat-top central part with  $TL2$  duration time sided by two sinusoidal-shaped rising and falling parts, each with  $TL1$  and  $TL3$  duration times. For our simulations, two finite laser pulses  $S1$  with  $TL2 = 80 \text{ fs}$  and  $TL1 = TL3 = 60 \text{ fs}$ , and  $S2$  with  $TL2 = 140 \text{ fs}$  and  $TL1 = TL3 = 30 \text{ fs}$  are typically selected. In our simulations, since the pulse lengths satisfy the condition  $L_p > \lambda_p^{NL}$  [ $\lambda_p^{NL}$  is the nonlinear plasma wavelength (Sprangle *et al.*, 1990)], they can cover a full plasma period leading to the pulse modulation during the propagation.

The electron energy spectrum is shown in Figure 1 at different times 240, 480, and 720 fs, for two pulses: (a)  $S1$  and (b)  $S2$ . It is observed that the maximum energy of electrons in the spectrum increases by increasing the interaction time for the two cases  $S1$  and  $S2$ . Furthermore, it is clear that there are fundamental differences between the two Figures (a) and (b). Though in the case  $S2$  [Fig. 1(b)] only the rise time of the laser pulse changes, but we can see a significant increase in energy levels of electrons compared with Figure 1(a). As shown, the maximum energy of electrons in the two cases  $S1$  and  $S2$  is 5.2 and 42.4 MeV, respectively. In addition, with increasing interaction time, the shape of distribution

function and mean broadening remain almost unchanged in Figure 1(a). This indicates that all electrons are affected by one acceleration mechanism and the temperature of electrons does not vary considerably over the time. This is while in Figure 1(b), at different interaction times, the different shapes and the different mean broadenings of the energy spectrum are perceptible. Therefore, the electrons energy is affected by the rise time of the laser pulse. Now, the key question is: What is the mechanism of the plasma electrons' acceleration, which leads to such varying spectra with the pulse rise time? In order to address this question, the longitudinal momentum, the transverse vector potential, and the longitudinal electric field versus  $x$  at different times (a)  $t = 240 \text{ fs}$ , (b)  $t = 480 \text{ fs}$  and (c)  $t = 720 \text{ fs}$  are plotted for the two pulses  $S1$  and  $S2$  in Figures 2 and 3, respectively. It is evident from Figure 2(a), during interaction progression; the chaos pattern appears as soon as the plasma response is taken into account. In this figure, because the rise time of the pulse is long, a weak ponderomotive force is produced according to the ponderomotive force relation:

$$F_p = -mc^2 \nabla \gamma \approx -mc^2 \nabla \left( 1 + \frac{a^2}{2} \right). \quad (5)$$

In Eq. (5),  $\gamma = (1 - v^2/c^2)^{-1/2}$  is the relativistic factor for electron. In this case, the amplitude of the longitudinal electric field (space-charge field) due to the weak ponderomotive force is relatively low. Therefore, the third item in Eq. (2) has a negligible portion. In this case, the scattered fields could have a major role in the appearing chaos (Khalilzadeh *et al.*, 2015). In fact, in this situation, bunching of the electrons weakens and the coupling of the electromagnetic waves with the electrostatic wave is fragile. When the amplitude of waves (main and scattered waves) pass the stochastic threshold amplitudes (Mendonca, 1983) pulse cannot scatter in the proper phase from these unreliable bunches. Simultaneously, these fragile bunches are broken down, the chaotic pattern appears. It should be noticed that by increasing the interaction time in sections (b) and (c), despite an increase in the electric field amplitude, this amplitude is not strong enough to establish a phase relation between electromagnetic waves, as a result the chaos happens. It is evident that with increasing interaction time in Figure 2(a)–2(c), the momentum space widens and the longitudinal momentum increases. This is consistent with the energy spectrum observed in Figure 1(a). As a result, in the pulse with the long rise time, during interaction time, all electrons obey from one acceleration mechanism which is stochastic acceleration because of the scattered fields generated in the plasma. Therefore, it is expectable that the shape of the electron energy spectrum remains stable in the different time steps. On the other hand, all of electrons are affected by several off-phase potentials in stochastic situation, and they are bounded and accelerated in the body of these potential waves. Then, the acceleration mechanism of the electrons is slow and

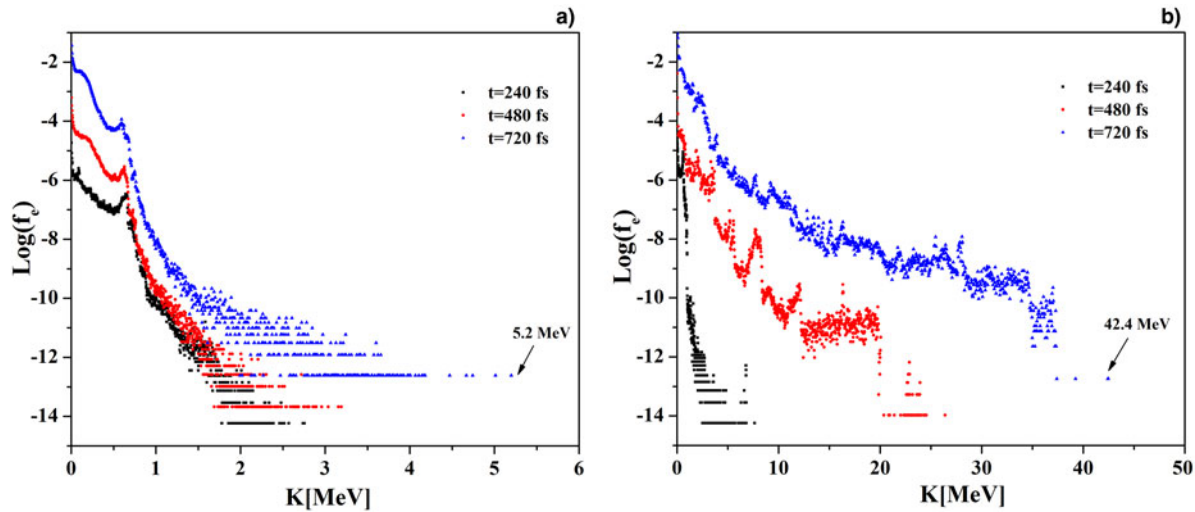


Fig. 1. The electron energy distribution function versus electron energy at different times 240, 480, and 720 fs, for the two pulses (a) S1 and (b) S2.

continues, and they cannot be accelerated to the very high-energy level over the time.

According to Figure 3(a), in the area of pulse no chaos takes place and consequently all trajectories are regular. This is while, in comparison with Figure 2(a), only the rise time of the pulse has been changed. In Figure 3(a), due to the short rise time, the amplitude of the space charge wave is higher in comparison with the results of Figure 2(a). This amplitude increases in the constant part of the pulse due to the pulse modulation. On the other hand, the modulation between the radiation waves and the scattered waves produces the strong ponderomotive force (Decker et al., 1996; Esarey et al., 1998) that can derive the strong plasma longitudinal electrostatic mode and bunch the electrons.

Therefore,  $\phi_w(x, t)$  has a large portion in Eq. (2) and the electrons are affected by it. In this case, the electrons sense a potential because of the modulation of the incident and scattered waves and show a regular pattern in the phase space with integrable Hamiltonian. It is evident that the amplitude of the plasma oscillations increases efficiently at the end of the pulse and the necessary condition for wave breaking is provided (Esarey et al., 1998). Another issue that needs to be considered is that the phase mixing discerned behind the pulse in the phase space is owing to the boundary effect. When the laser pulse is propagating in the plasma, due to the inhomogeneity of the density (Langmuir frequency) on the vacuum-plasma surface, the wake wave breaks and makes possible to inject electrons into the acceleration phase

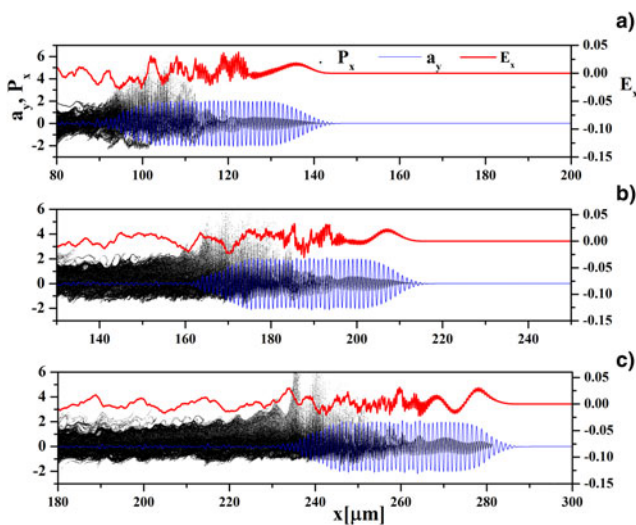


Fig. 2. The electron longitudinal momentum (left axis), the transverse vector potential (left axis), the longitudinal electric field (right axis) versus  $x$ , at different times (a) 240 fs, (b) 480 fs, and (c) 720 fs, for the pulse S1.

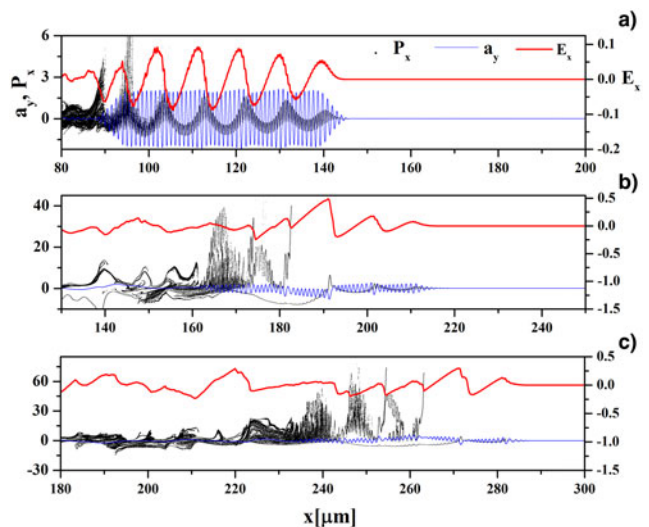
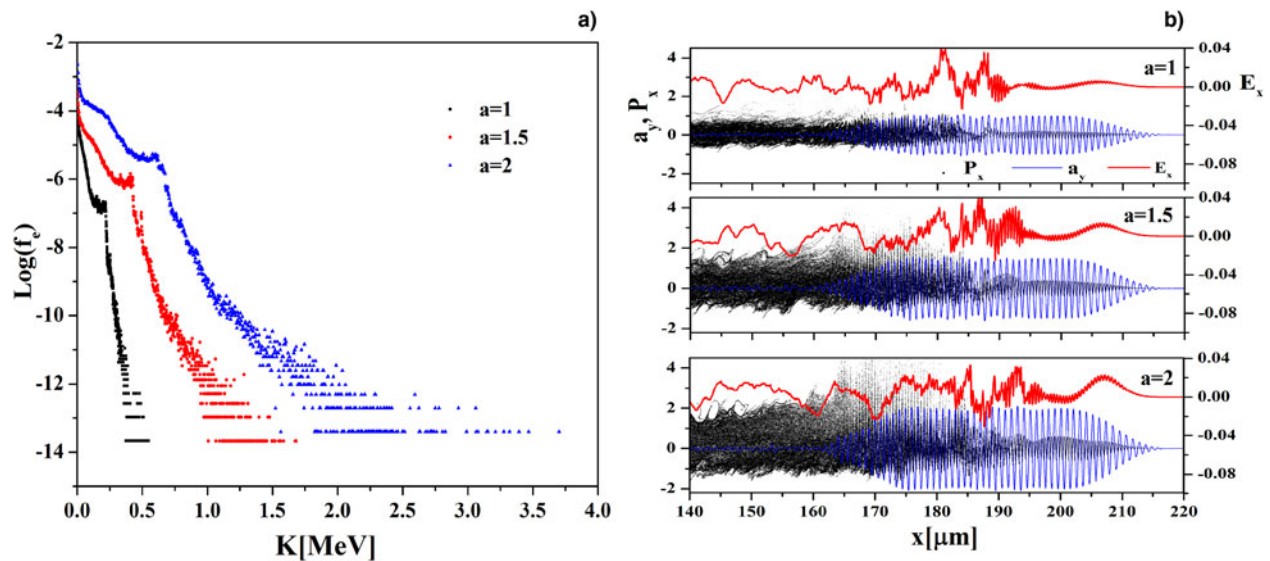


Fig. 3. The electron longitudinal momentum, the transverse vector potential, the longitudinal electric field at different times (a), (b) 480 fs, and (c) 720 fs, for the pulse S2.



**Fig. 4.** (a) The electron energy distribution function versus electron energy (b) The electron longitudinal momentum, the transverse vector potential, and the longitudinal electric field versus  $x$  for  $n = 0.02 n_{cr}$  at time  $t = 480$  fs and at the different amplitudes  $a = 1$ ,  $a = 1.5$ , and  $a = 2$  for the pulse S1.

of the wave (Bulanov *et al.*, 1998). This nonlinear wave breaking produces the electrons with high velocity near the pulse group velocity. In this case, the high-energy electron beam is generated. This beam derived a new electrostatic mode that does not have any relation phase with the space charge electrostatic mode. As a result, an off-phase potential,  $\varphi_{th}(x, t)$ , can destroy the regular structure of the wave behind the laser pulse and create chaos. It is expected with moving away from the vacuum-plasma boundary, this effect weakens. By increasing the interaction time in sections (b) and (c), the most interesting mechanism happens. Paying detailed attention to these sections, we can realize that due to the high electrostatic field, the wave breaking occurs faster than section (a). The electrons produced because of the wave breaking leads to two different configurations in the phase space. The first configuration consists of the energetic electrons released owing to the wave breaking and so, they undergo the direct laser acceleration mechanism (Li *et al.*, 2011; Shaw *et al.*, 2014; Zhang *et al.*, 2015). The second type belongs to the electrons whose trajectories in the phase space are irregular. These electrons are in the body of the broken longitudinal wave. Hence, due to this wave breaking, laminar motion of the layers in the phase space is broken down and the layers are mixed. The electrons in the body of the mixed layers represent chaotic pattern in the phase space and their trajectories in the phase space are irregular.

In the pulse with short rise time, three acceleration mechanisms take place over the time: first, stochastic mechanism initiated by the longitudinal space charge wave breaking; second, direct laser acceleration of the released electrons; and third, chaotic mechanism originated from the nonlinear wave breaking via plasma-vacuum boundary effect. Under these conditions, it is expectable that the phase space pattern

and the shape and mean broadening of the energy spectrum change over the time. As a result, when the rise time of the pulse is short, chaos mechanism is established due to the space-charge wave breaking. Some of the electrons released owing to the wave breaking, are directly accelerated to the very high energies by the laser pulse field. These electrons remain in the tail part of the electron distribution function over time. Beside this mechanism, after the wave breaking, several incoherent longitudinal waves or potentials affect some of the electrons. Depending on the initial conditions, the electron chooses one of these different paths. In this case, the electrons trajectory in the phase space is irregular and acceleration of electrons to much higher energy is possible. Therefore, the high-energy electrons observed in Figure 1(b) are free electrons produced via direct laser acceleration and stochastic acceleration.

#### 4. PARAMETRIC ANALYSES

It is evident that the strength and phase of each potential in Eq. (1) depend largely on the initial condition. Therefore, the stochastic acceleration can be highly sensitive to the initial laser and plasma parameters. Hence, in order to understand the relation between the energy of electrons and the different parameters, different simulations based on the PIC simulation are performed by varying the laser intensity and the plasma density for the two finite laser pulses S1 and S2, in the following procedure.

To show the influence of variation in pulse intensity and plasma density on the electron energy, the energy spectrum and momentum phase are illustrated in detail in Figures 4 and 5 for the pulse S1. Figure 4, illustrates the maximum electron energy that is 0.5 MeV for  $a = 1$ , reach 1.6 MeV

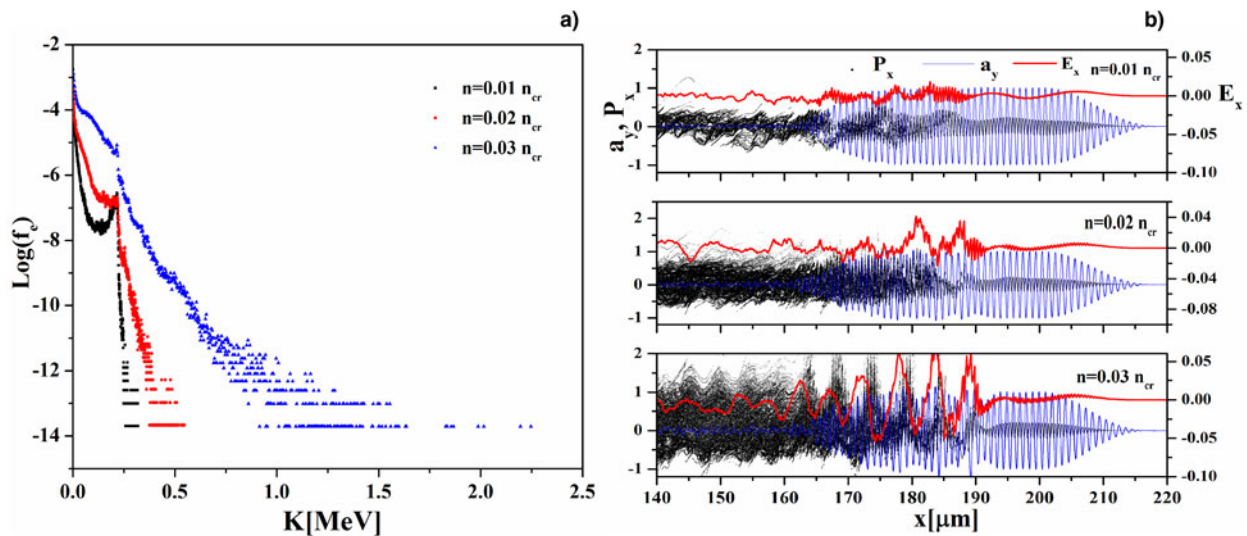


**Fig. 5.** (a) The electron energy distribution function versus electron energy and (b) The electron longitudinal momentum, the transverse vector potential, and the longitudinal electric field versus  $x$  for  $a = 1$  at time  $t = 480$  fs and at different densities  $n = 0.01 n_{cr}$ ,  $n = 0.02 n_{cr}$ , and  $n = 0.03 n_{cr}$  for the pulse S1.

when the laser pulse intensity is increased to  $a = 1.5$ . This increase continues with the increase in pulse intensity such that when  $a = 2$ , the maximum energy of the electron reaches 3.7 MeV. Also, as shown in Figure 5, with an increase in electron density from  $n = 0.01 n_{cr}$  to  $n = 0.02 n_{cr}$  and  $n = 0.03 n_{cr}$ , the maximum energy of the electrons increase and take the values 0.3, 0.5, and 2.25 MeV, respectively. In the light of Figures 4 and 5, it is found that by increasing the pulse intensity and electron density for the pulse with the rise time 60 fs, the shape of distribution function is maintained. This indicates that the acceleration mechanism of electrons does not change by changing the laser and plasma parameters. This is consistent with the phase space diagram

in Figures 4 and 5 that show despite the increase in the electric field amplitude due to the increase in the pulse amplitude and the plasma density, the electric field amplitude is not strong enough to establish a phase relation between electromagnetic waves. Therefore, with a slight increase in the pulse amplitude and the plasma density, the width of the stochastic pattern in the phase space increases and the electrons can reach higher energy.

In Figures 6 and 7, the energy spectrum and the electron phase space are shown in detail for the pulse S2. It is evident from Figure 6 that when the pulse intensity amplitude increases, the electrons energy in the spectrum increases such that for  $a = 1$ , 1.5, and 2, the maximum energy of the

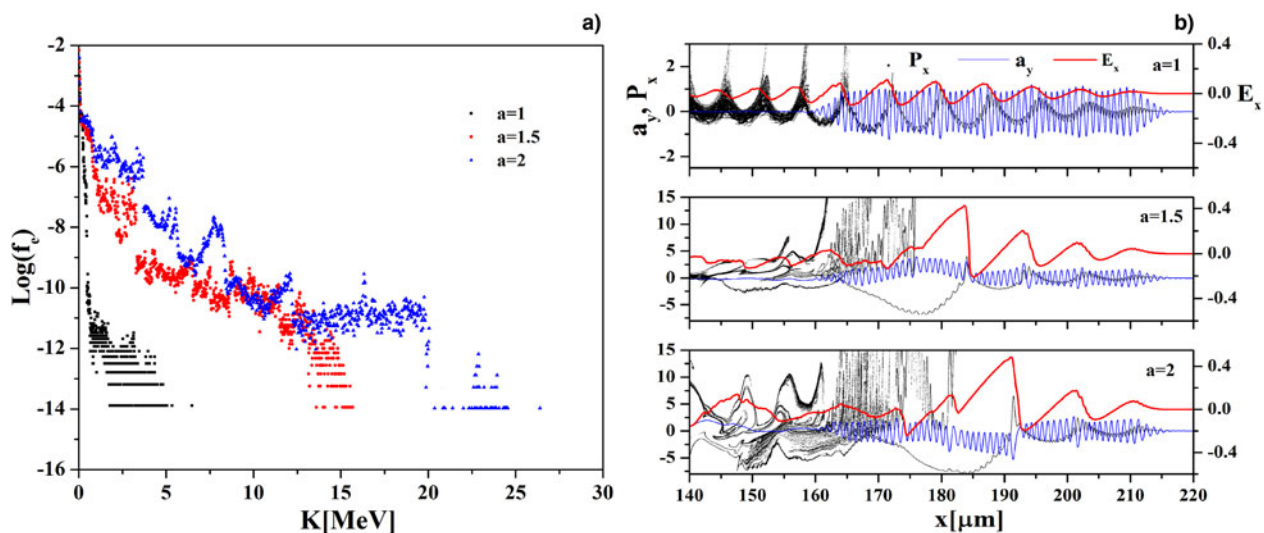


**Fig. 6.** (a) The electron energy distribution function versus electron energy and (b) The electron longitudinal momentum, the transverse vector potential, and the longitudinal electric field versus  $x$  for  $n = 0.02 n_{cr}$  at time  $t = 480$  fs and at the different amplitudes  $a = 1$ ,  $a = 1.5$ , and  $a = 2$  for the pulse S2.

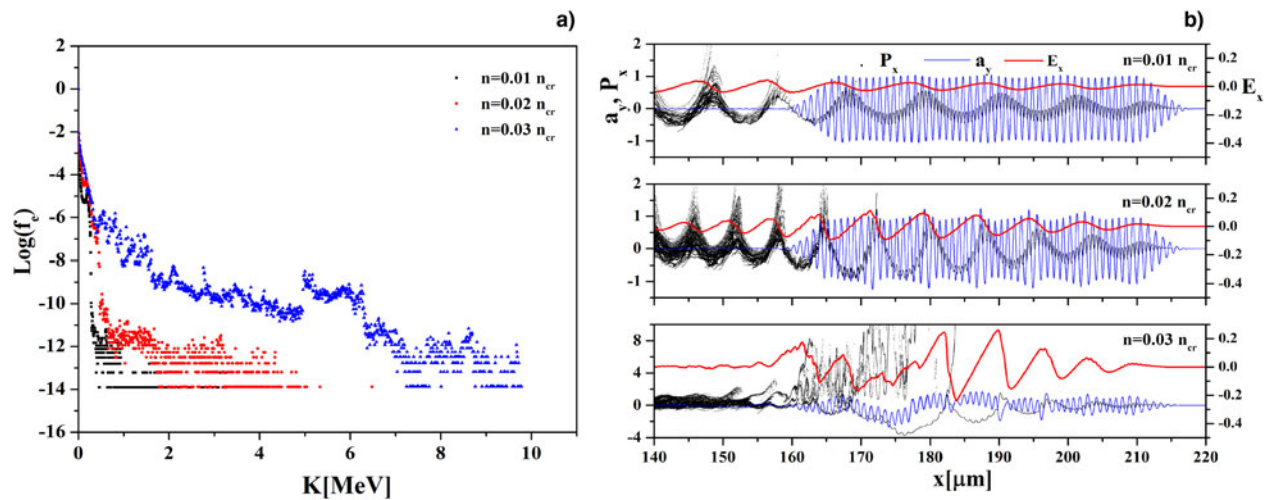


**Fig. 7.** (a) The electron energy distribution function versus electron energy and (b) The electron longitudinal momentum, the transverse vector potential, and the longitudinal electric field versus  $x$  for  $a = 1$  at time  $t = 480$  fs and at different densities  $n = 0.01 n_{cr}$ ,  $n = 0.02 n_{cr}$ , and  $n = 0.03 n_{cr}$  for the pulse S2.

electrons reaches the value 6.4, 15.7, and 26.3 MeV, respectively. Also, the shape of distribution function varies by changing the laser pulse intensity. It is attributed to this fact that the acceleration mechanism of the electrons is different in three intensities. As shown in phase space diagram, for  $a = 1$ , the wave breaking due to increasing the amplitude of the electric field is the only mechanism for generation of the high-energy electron. For  $a = 1.5$  and 2, after the wave is broken, laminar motion of the layers in phase space starts to mix and then stochastic pattern in the motion of some electrons is appeared. However, some of the electrons can be released due to the wave breaking and accelerate directly in the laser field. These two types of electrons with their high energy are distinguishable in the electron energy spectrum. Also, as shown in Figure 7, the electrons energy grows with increasing the plasma density. The maximum electron energies increase from 3.3, 6.4, and 9.7 MeV, as the electron density increase from  $n = 0.01 n_{cr}$  to  $n = 0.02 n_{cr}$  and  $n = 0.03 n_{cr}$ , respectively. According to the changes in the shape of the distribution function in the different plasma densities, the electrons are expected to accelerate by different mechanisms, as mentioned previously. As shown in phase space diagram, for  $n = 0.01 n_{cr}$  the nonlinear wave breaking originated from inhomogeneity of the density on the vacuum-plasma surface is the only mechanism for generation of the high-energy electron. For  $n = 0.02 n_{cr}$ , the wave breaking due to increasing the electric field amplitude produces the high-energy electrons; and for  $n = 0.03 n_{cr}$ , two types of high-energy electrons with two action types are seen in the phase space; in the one type the electrons motion is regular (direct acceleration) and in the other type, the electrons motion is chaotic (stochastic acceleration).

In the end, the simulation results in Figures 4–7 show that the electrons energy will considerably be changed by

applying a minor change to the initial laser or plasma parameters. This is consistent with chaotic nature of the motion.

## 5. CONCLUSION

By the use of PIC simulation, the energy distribution function of electrons in the interaction of the underdense plasma with ultrashort laser pulse is studied. It is found that different chaotic mechanisms can affect this energy spectrum.

The result of our simulations shows that in respect to the short rise time, electrons are accelerated to higher energy level than the case with the long rise time. Time evolution study of the energy distribution function indicates that with the time progressing of the pulse propagation, in the shorter rise time case electrons can reach energies about eight times higher than the electron energy level of the case with the longer rise time, in spite of the fact that the rise time of the pulse is doubled. On the other hand, the energy spectrum shape and mean broadening, in the longer rise time case, are unchanged over the time approximately. This is a proof that in the interaction of the plasma with the long rise time laser pulse all electrons are affected by the one acceleration mechanism and temperature of electrons does not vary considerably over the time. In this case, the scattered wave amplitude and the amplitude of the incident wave can satisfy Mendonca stochastic criteria (Mendonca, 1983), as two counter-propagate waves, and electrons are accelerated via this chaos mechanism. If the rise time of the pulse is short, chaos mechanism is established due to the space-charge wave breaking. Under this condition, several incoherent longitudinal waves or potentials, after wave breaking, affect the electrons. These incoherent longitudinal waves on the one hand can accelerate electrons and on the other hand can

heat the electrons considerably, via some mechanisms such as nonlinear Landau damping, over the time. On the other point of view, some of the electrons which are released owing to the wave breaking, are directly accelerated to the very high energies by the laser pulse field. These electrons remain in the tail part of the electron distribution function over time. In this situation, as regards to the short rise time pulse, three mechanisms take place: first, stochastic mechanism initiated by the longitudinal space charge wave breaking; second, direct laser acceleration of the released electrons; and the third, chaotic mechanism originated from the nonlinear wave breaking via plasma-vacuum boundary effect. Therefore, the phase space pattern and the shape and mean broadening of the energy spectrum change over the time.

Parametric analyses show that in the both cases, short and long rise time pulses, increment of the laser amplitude and the plasma density increase the electrons energies. In the pulse with the longer rise time, when the pulse amplitude is doubled the maximum energy of the electrons grows seven times but the mean distribution broadening is approximately doubled. However, when the plasma density is tripled, variation in the mean distribution broadening is not perceivable, but the tail of the electrons spectral energy extends nearly seven times. On the other hand, when the pulse with the shorter rise time interacts with the plasma, about one order of magnitude increment in the electrons energy level is discernible. Additionally, in this case the same as the previous case when the pulse amplitude is doubled, the maximum energy of the electrons grows seven times, but the mean distribution broadens virtually ten times. Finally, when the plasma density is tripled, the mean distribution broadening is doubled but the spectral energy tail of the electrons extends about five times.

## REFERENCES

- ADAM, J.C., HÉRON, A., GUÉRIN, S., LAVAL, G., MORA, P. & QUESNEL, B. (1997). Anomalous absorption of very high-intensity laser pulses propagating through moderately dense plasma. *Phys. Rev. Lett.* **78**, 4765–4768.
- BAUER, D., MULSE, P. & STEEB, W.H. (1995). Relativistic ponderomotive force, uphill acceleration, and transition to chaos. *Phys. Rev. Lett.* **75**, 4622–4625.
- BULANOV, S., NAUMOVA, N., PEGORARO, F. & SAKAI, J. (1998). Particle injection into the wave acceleration phase due to nonlinear wake wave breaking. *Phys. Rev. E* **58**, R5257.
- DECKER, C.D., MORI, W.B., TZENG, K.C. & KATSIOULEAS, T. (1996). The evolution of ultra-intense, short-pulse lasers in underdense plasmas. *Phys. Plasmas* **3**, 2047–2056.
- ESAREY, E., HAFIZI, B., HUBBARD, R. & TING, A. (1998). Trapping and acceleration in self-modulated laser wakefields. *Phys. Rev. Lett.* **80**, 5552–5555.
- ESCANDE, D.F. & DOVEIL, F. (1981). Renormalization method for the onset of stochasticity in a Hamiltonian system. *Phys. Lett. A* **83**, 307–310.
- JACKSON, J.D. (1962). *Classical Electrodynamics*, 3rd Edition. New York: John Wiley & Sons Ltd.
- KHALILZADEH, E., YAZDANPANA, J., JAHANPANA, J. & CHAKHMACHI, A. (2016). Numerical modeling of radiative recombination during ionization of atoms by means of particle-in-cell simulation. *Laser Part. Beams* **34**, 284–293.
- KHALILZADEH, E., YAZDANPANA, J., JAHANPANA, J., CHAKHMACHI, A. & YAZDANI, E. (2015). Electron residual energy due to stochastic heating in field-ionized plasma. *Phys. Plasmas* **22**, 113115.
- LI, Y.Y., GU, Y.J., ZHU, Z., LI, X.F., BAN, H.Y., KONG, Q. & KAWATA, S. (2011). Direct laser acceleration of electron by an ultra intense and short-pulsed laser in under-dense plasma. *Phys. Plasmas* **18**, 053104.
- LICHTENBERG, A.J. & LIEBERMAN, M.A. (1981). *Regular and Stochastic Motion*. New York: Springer-Verlag.
- LITOS, M., ADLI, E., AN, W., CLARKE, C.I., CLAYTON, C.E., CORDE, S., DELAHAYE, J.P., ENGLAND, R.J., FISHER, A.S., FREDERICO, J., GESSNER, S., GREEN, S.Z., HOGAN, M.J., JOSHI, C., LU, W., MARSH, K.A., MORI, W.B., MUGGLI, P., VAFAEI-NAJAFABADI, N., WALZ, D., WHITE, G., WU, Z., YAKIMENKO, V. & YOCKY, G. (2014). High-efficiency acceleration of an electron beam in a plasma wakefield accelerator. *Nature* **515**, 92–95.
- MENDONCA, J.T. (1983). Threshold for electron heating by two electromagnetic waves. *Phys. Rev. A* **28**, 3592–3598.
- MOUROU, G., BARTY, C.P.J. & PERRY, M.D. (1998). Ultrahigh-intensity lasers: Physics of the extreme on a tabletop. *Phys. Today* **51**, 22–28.
- PARADKAR, B.S., WEI, M.S., YABUCHI, T., STEPHENS, R.B., HAINES, M.G., KRASHENINNIKOV, S.I. & BEG, F.N. (2011). Numerical modeling of fast electron generation in the presence of preformed plasma in laser-matter interaction at relativistic intensities. *Phys. Rev. E* **83**, 046401.
- SARACHIK, E.S. & SCHAPPERT, G.T. (1970). Classical theory of the scattering of intense laser radiation by free electrons. *Phys. Rev. D* **1**, 2738–2753.
- SHAW, J.L., TSUNG, F.S., VAFAEI-NAJAFABADI, N., MARSH, K.A., LEMOS, N., MORI, W.B. & JOSHI, C. (2014). Role of direct laser acceleration in energy gained by electrons in a laser wakefield accelerator with ionization injection. *Plasma Phys. Contr. Fusion* **56**, 084006.
- SHENG, Z.M., MIMA, K., SENTOKU, Y., JOVANOVIĆ, M.S., TAGUCHI, T., ZHANG, J. & MEYER-TER-VEHN, J. (2002). Stochastic heating and acceleration of electrons in colliding laser fields in plasma. *Phys. Rev. Lett.* **88**, 055004.
- SHENG, Z.M., MIMA, K., ZHANG, J. & MEYER-TER-VEHN, J. (2004). Efficient acceleration of electrons with counterpropagating intense laser pulses in vacuum and underdense plasma. *Phys. Rev. E* **69**, 016407.
- SMITH, G.R. & KAUFMAN, A.N. (1975). Stochastic acceleration by a single wave in a magnetic field. *Phys. Rev. Lett.* **34**, 1613–1616.
- SPRANGLE, P., ESAREY, E. & TING, A. (1990). Nonlinear theory of intense laser-plasma interaction. *Phys. Rev. Lett.* **64**, 2011–2014.
- STRICKLAND, D. & MOUROU, G. (1985). Compression of amplified chirped optical pulses. *Opt. Commun.* **56**, 219–221.
- TING, A., MOORE, C.I., KRUSHELNICK, K., MANKA, C., ESAREY, E., SPRANGLE, P., HUBBARD, R., BURRIS, H.R., FISCHER, R. & BAINE, M. (1997). Plasma wakefield generation and electron acceleration in a self-modulated laser wakefield accelerator experiment. *Phys. Plasmas* **4**, 1889–1899.
- TZENG, K.C., MORI, W.B. & KATSIOULEAS, T. (1997). Electron beam characteristics from laser-driven wave breaking. *Phys. Rev. Lett.* **79**, 5258–5261.

- YAZDANI, E., SADIGHI-BONABI, R., AFARIDEH, H., YADANPANA, J. & HORA, H. (2014). Enhanced laser ion acceleration with a multi-layer foam target assembly. *Laser Part. Beams* **32**, 509–515.
- YAZDANPANA, J. & ANVARY, A. (2012). Time and space extended-particle in cell model for electromagnetic particle algorithms. *Phys. Plasmas* **19**, 033110.
- YAZDANPANA, J. & ANVARY, A. (2014). Effects of initially energetic electrons on relativistic laser-driven electron plasma waves. *Phys. Plasmas* **21**, 023101.
- ZHANG, P., SALEH, N., CHEN, C., SHENG, Z.M. & UMSTADTER, D. (2003a). Laser-energy transfer and enhancement of plasma waves and electron beams by interfering high-intensity laser pulses. *Phys. Rev. Lett.* **91**, 225001.
- ZHANG, P., SALEH, N., CHEN, C., SHENG, Z.M. & UMSTADTER, D. (2003b). An optical trap for relativistic plasma. *Phys. Plasmas* **10**, 2093–2099.
- ZHANG, X., KHUDIK, V.N. & SHVETS, G. (2015). Synergistic laser-wakefield and direct-laser acceleration in the plasma-bubble regime. *Phys. Rev. Lett.* **114**, 184801.